

DYNAMIC STABILITY OF THE PERIODIC AND APERIODIC STRUCTURES OF THE BERNOULLI-EULER BEAMS

The study analyzed the influence of periodic and aperiodic stiffness distribution for the four-element Bernoulli-Euler beam on the first two eigenfrequencies and the dynamic stability of the system. The influence of increasing the ratio of cross-sections of the analyzed elements was also analyzed. Significant differences were found in eigenfrequencies and dynamic stability. Using the variational Hamilton principle, the equation of motion was derived, on the basis of which the values of the eigenfrequencies were determined, and the transformation into the form of the Mathieu equation made it possible to determine the dynamic stability for the analyzed structures.

Keywords: Beam; dynamic stability; Mathieu equation; aperiodic structure

1. Introduction

Columns are widely used in structures and mechanical devices, moreover, many design problems can be traced back to the analysis of basic elements such as columns. The analysis of the column's own vibrations and the analysis of the vibrations resulting from the action of a relatively small force changing in time allow to determine for which material and geometric parameters the system may become unstable, and thus be destroyed. It can be assumed that the construction of the column from elements with irregular order will significantly affect the phenomenon of parametric resonance, which may allow for the design of safer structures. In addition, adding elements to the existing column that change its geometry will affect its natural frequencies and dynamic stability.

The well-known phenomenon of parametric resonance can be observed in a wide variety of optical, mechanical, electrical, and physical systems [1-5]. Parametric resonance can be observed in mechanical systems such as, for example, by applying an axial load to a cantilever beam [3,6], or it can even result from changes in stiffness [7]. Parametric resonance can be analyzed by reducing the equation of motion of the system to the form of the Mathieu equation [8-13]. Periodic solutions of the Mathieu equation allow to designate areas of stable and

unstable solutions [14]. The paper [15] presents the results of the homogeneous Mathieu equation, where the dependencies of the oscillation data on the ratio of the coefficients were found. These dependencies can be used to approximate the solutions of the Mathieu equation without integration. In the paper [12] the dynamic stability of a simply supported beam with additional discrete elements such as a concentrated mass, an undamped harmonic oscillator and an elastic spring was investigated. Dynamic stability studies were also carried out using the Mathieu equation for much more complex systems, such as the truck crane [9]. In the works [16,17], the dynamic stability of a beam built of materials of different stiffness was investigated. The dynamic stability of micro and nanobeams was also investigated [18-20]. In [21] the material with axially continuous gradual variation properties was considered. So far, research has been carried out on the dynamic stability of plates with variable stiffness [22], but the influence of variable stiffness with aperiodic distribution in the beam is unknown.

The work will investigate the impact of the stiffness distribution in the Bernoulli-Euler beam on the eigenfrequency values and the dynamic stability of the analyzed structures. The variable stiffness of the column results from the multiple step change of the geometrical and material parameters of its individual segments. It is assumed that different types of stiffness distribution

¹ CZESTOCHOWA UNIVERSITY OF TECHNOLOGY, DEPARTMENT OF MECHANICS AND MACHINE DESIGN FUNDAMENTALS, FACULTY OF MECHANICAL ENGINEERING AND COMPUTER SCIENCE, 73 DĄBROWSKIEGO STR., 42-201 CZĘSTOCHOWA, POLAND

² VSB-TECHNICAL UNIVERSITY OF OSTRAVA, FACULTY OF MECHANICAL ENGINEERING DEPARTMENT OF MACHINING, ASSEMBLY AND ENGINEERING METROLOGY, 70833 OSTRAVA, CZECH REPUBLIC

* Corresponding author: sebastian.garus@pcz.pl



in a column (periodic or aperiodic) with given geometric and material properties will significantly affect the values of the natural frequencies of the analyzed columns, as well as, in the case of a force variable in time, on their dynamic stability.

Understanding the behavior of multi-segment Bernoulli-Euler columns, where the distribution of the stiffness in the column is periodic or aperiodic may be very important in the design of machines and devices where such columns are used (e.g. bridges, storage halls). Knowledge about the influence of the distribution of various types of segments on the frequency of natural vibrations and dynamic stability will allow to avoid the phenomenon of parametric resonance and thus increase the safety of users.

2. Mathematical background

In this work, a multi-segment Bernoulli-Euler column, freely supported, loaded by a longitudinal force was considered. The problem of dynamic stability was solved using the mode summation method. The applied research procedure allow the dynamics of the tested system to be described with the use of the Mathieu equation. The influence of stiffness distribution in the Bernoulli-Euler column on the first and second eigenfrequency and the dynamic stability of the system was investigated.

Fig. 1 shows a Bernoulli-Euler column, hinged at its ends, loaded with an axial compressive force as described by the relation $P(t) = P_0 + S \cos \nu t$, where P_0 is a constant component of the load, S is a variable component of the load, ν is the frequency of the exciting force, and t determines the time. The material property of the beam is the Young's modulus E_i , section moment of inertia J_i , cross-sectional area A_i and the density of the material ρ_i .

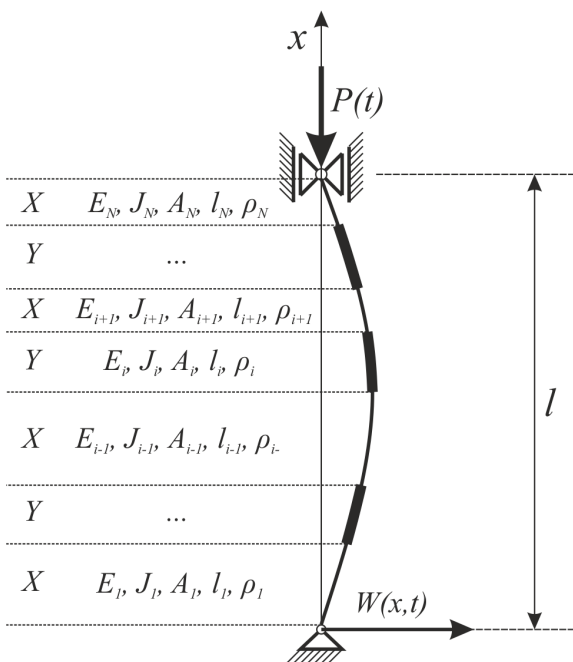


Fig. 1. Multi-segment Bernoulli-Euler column loaded with an axial compressive force that changes cyclically

The problem of transverse vibrations of multi-segment Bernoulli-Euler column was solved by formulating the boundary problem using the Hamilton variational principle

$$\delta \int_{t_1}^{t_2} (T - V) dt = 0 \tag{1}$$

Kinetic energy T was defined as

$$T = \sum_{i=1}^N \frac{1}{2} \int_0^l \rho_i A_i \left(\frac{\partial W_i(x,t)}{\partial t} \right)^2 dx \tag{2}$$

The variation of kinetic energy was determined using the alternation of the integration operation with respect to time and space variables and using integration by parts. For $t = t_1$ and $t = t_2$ the value of the variation $\delta W_i(x,t)$ is equal to zero, substituting we get

$$\delta T = - \sum_{i=1}^N \left[\int_0^l \rho_i A_i \frac{\partial^2 W_i(x,t)}{\partial t^2} \delta W_i(x,t) dx \right] \tag{3}$$

Potential energy of the system $V = V_1 + V_2$ was defined as the sum of the bending spring energy for each i -th segment

$$V_1 = \sum_{i=1}^N \frac{1}{2} \int_0^l E_i J_i \left(\frac{\partial^2 W_i(x,t)}{\partial x^2} \right)^2 dx \tag{4}$$

and energy from an external load

$$V_2 = - \sum_{i=1}^N \frac{1}{2} P(t) \int_0^l \left(\frac{\partial W_i(x,t)}{\partial x} \right)^2 dx \tag{5}$$

Their variations are respectively

$$\delta V_{i,1} = \sum_{i=1}^N \left[\begin{aligned} & E_i J_i \frac{\partial^2 W_i(l,t)}{\partial x^2} \delta \frac{\partial W_i(l,t)}{\partial x} - \\ & E_i J_i \frac{\partial^2 W_i(0,t)}{\partial x^2} \delta \frac{\partial W_i(0,t)}{\partial x} - \\ & E_i J_i \frac{\partial^3 W_i(l,t)}{\partial x^3} \delta W_i(l,t) + \\ & E_i J_i \frac{\partial^3 W_i(0,t)}{\partial x^3} \delta W_i(0,t) + \\ & \int_0^l E_i J_i \frac{\partial^4 W_i(x,t)}{\partial x^4} \delta W_i(x,t) dx \end{aligned} \right] \tag{6}$$

$$\delta V_{i,2} = \sum_{i=1}^N \left[\begin{aligned} & \int_0^l P(t) \frac{\partial^2 W_i(x,t)}{\partial x^2} \delta W_i(x,t) dx - \\ & P(t) \frac{\partial W_i(l,t)}{\partial x} \delta W_i(l,t) + \\ & P(t) \frac{\partial W_i(0,t)}{\partial x} \delta W_i(0,t) \end{aligned} \right] \tag{7}$$

The equations of motion of the column transverse vibrations was determined as

$$\frac{\partial^4 W_i(x,t)}{\partial x^4} + \frac{P(t)}{E_i J_i} \frac{\partial^2 W_i(x,t)}{\partial x^2} + \frac{\varrho_i A_i}{E_i J_i} \frac{\partial^2 W_i(x,t)}{\partial t^2} = 0 \quad (8)$$

The solution of equation (8) is predicted as a series of eigenfunctions

$$W_i(x,t) = \sum_{n=1}^{\infty} W_{i,n}(x) T_{i,n}(t) \quad (9)$$

where $W_{i,n}(x)$ is the n -th free vibration form of the i segment, and $T_{i,n}(t)$ is an unknown function of time.

For the first form of vibrations, displacement $W_i(x,t)$ is written as a product of functions with variables separated by time t and coordinate x

$$W_i(x,t) = W_i(x)T(t) = W_i(x) \cos \omega_{i,1}t \quad (10)$$

Substituting $d_i^2 = \frac{P(t)}{E_i J_i}$ and $\Omega_i^2 = \frac{\varrho_i A_i \omega_{i,1}^2}{E_i J_i}$ we get

$$\frac{\partial^4 W_i(x)}{\partial x^4} + d_i^2 \frac{\partial^2 W_i(x)}{\partial x^2} - \Omega_i^2 W_i(x) = 0 \quad (11)$$

For the system shown in Fig. 1, the geometric boundary conditions after separating the variables are

$$W_1(0) = W_N(l) = 0 \quad (12)$$

The natural boundary conditions after separating the variables are determined

$$E_i J_i \frac{d^2 W_N(l)}{dx^2} = 0 \quad (13)$$

$$E_i J_i \frac{d^2 W_1(0)}{dx^2} = 0 \quad (14)$$

The conditions of continuity between regions of variable stiffness were defined as

$$W_i(x) = W_{i+1}(x) \quad (15)$$

$$\frac{dW_i(x)}{dx} = \frac{dW_{i+1}(x)}{dx} \quad (16)$$

$$E_i J_i \frac{d^2 W_i(x)}{dx^2} = E_{i+1} J_{i+1} \frac{d^2 W_{i+1}(x)}{dx^2} \quad (17)$$

$$E_i J_i \frac{d^3 W_i(x)}{dx^3} = E_{i+1} J_{i+1} \frac{d^3 W_{i+1}(x)}{dx^3} \quad (18)$$

The general solution to the displacement equation (11) is a function

$$W_i(x) = C_{i,1} \cosh(\alpha_i x) + C_{i,2} \sinh(\alpha_i x) + C_{i,3} \cos(\beta_i x) + C_{i,4} \sin(\beta_i x) \quad (19)$$

where

$$\alpha_i = \sqrt{-\frac{1}{2}d_i^2 + \sqrt{\frac{1}{4}d_i^4 + \Omega_i^2}} \quad (20)$$

$$\beta_i = \sqrt{\frac{1}{2}d_i^2 + \sqrt{\frac{1}{4}d_i^4 + \Omega_i^2}} \quad (21)$$

By inserting solution (19) and its derivatives into equations (12)-(18), a homogeneous system of equations M was obtained with respect to the unknown constants $C_{i,j}$. This matrix system is written as $[M](\omega)C = 0$, where $[M](\omega)C = [a_{pq}]; [p, q] = (1-4)$, and $C = [C_i]^T; i = 1-N; j = 1-4$.

In the case when the determinant of the matrix of coefficients is equal to zero with the constants C_i , the system has a non-trivial solution. Equation $(\det M(\omega) = 0)$ allows to determine the dependence of the eigenfrequencies of the system ω_i from the load P and determine the critical load value P_k .

To expand eigenfunctions in series (9) their orthogonality is assumed. Equation (11) after separating the variables for the n -th and m -th eigenfunctions and taking into account the boundary conditions (12)-(14) and simplifying, we obtained

$$\sum_{i=1}^N \left[\varrho_i A_i (\omega_{i,m}^2 - \omega_{i,n}^2) \int_0^l W_{i,n}(x) W_{i,m}(x) dx \right] = 0 \quad (22)$$

Because $\omega_{i,m} \neq \omega_{i,n}$, when $m \neq n$, then

$$\sum_{i=1}^N \left[\varrho_i A_{ii} \int_0^l W_{i,n}(x) W_{i,m}(x) dx \right] = \begin{cases} 0 & m \neq n \\ \gamma_m^2 = \sum_{i=1}^N \left[\int_0^l W_i^2(x) dx \right] & m = n \end{cases} \quad (23)$$

The orthogonality condition sought is determined by the formula (23).

Substituting equation (9) into equation (11) and taking into account the orthogonality condition and substituting $\tau = vt$, the equation of motion in the form of the Mathieu equation

$$\frac{\partial^2 T(\tau)}{\partial \tau^2} + (a + b \cos \tau) T(\tau) = 0 \quad (24)$$

and was obtained as

$$\frac{\partial^2 T(\tau)}{\partial \tau^2} + \left(\frac{-\omega_i^2}{v^2} + \frac{\sum_{i=1}^N \int_0^l \frac{\partial^2 W_i(x)}{\partial x^2} W_i(x) dx}{\sum_{i=1}^N \varrho_i A_i \int_0^l W_i^2(x) dx} \frac{S}{v^2} \cos \tau \right) T(\tau) = 0 \quad (25)$$

where

$$a = \frac{-\omega_i^2}{v^2} \quad (26)$$

$$b = b_1 \frac{S}{v^2} = \frac{\sum_{i=1}^N \int_0^l \frac{\partial^2 W_i(x)}{\partial x^2} W_i(x) dx}{\sum_{i=1}^N \rho_i A_i \int_0^l W_i^2(x) dx} \frac{S}{v^2} \quad (27)$$

The numerical values of the parameters a and b each time decide whether the solution lies in a stable or unstable area.

3. Research

A binary structure will be used as an example of a periodic structure [23]. For the initial value $a_0 = XY$, the successive steps are described by the formula (28), where the superscript denotes the number of times the sequence is repeated, and the parameters X and Y symbolize a given type of Bernoulli-Euler segment.

$$a_n = (a_0)^n \quad (28)$$

The Thue-Morse chain [24-28] was used as the aperiodic structure. The Thue-Morse chain for the initial values

$$\begin{cases} a_0 = X \\ a_1 = XY \end{cases} \quad (29)$$

is formed based on the substitution rule

$$\begin{cases} Y \rightarrow YX \\ X \rightarrow XY \end{cases} \quad (30)$$

Based on the above rules, subsequent types of beam distribution in the column are obtained.

The beams with periodic (binary – XYXY) and aperiodic (Thue-Morse – XYYX) stiffness distributions were analyzed. As can be seen, these are simple four-element structures with the same number of X and Y elements. The same mass. The length of the beam was assumed for the calculations, equal to 3 m. The length of the column segments was equal to the fourth part of its length. The entire column was made of a homogeneous material – steel (Young's modulus $E = 2.1 \cdot 10^{11}$ Pa, density $\rho = 7.86 \cdot 10^3$ kg · m⁻³). The static part and the variable part of the load were 5% of the critical load $P_C = 9.33 \cdot 10^7$ N. The cross-section of the segment X was a square with a side of 0.3 m with an area A_X . The cross-section of the segment Y was a square whose cross-sectional area A_Y was changed from the value equal to the area A_X to its four times.

Fig. 2 and Fig. 3 show the effect of increasing the cross-section A_Y in relation to A_X on the first and second eigenfrequencies, respectively. For the XYXY structure, the first eigenfrequency was smaller than for the XYYX structure over the entire analyzed range. For the ratio of the cross-sectional area of sections A_Y to A_X equal to 1.9, there was a maximum of the first eigenfrequency of 513.26 rad/s (XYXY structure). The maximum in the XYYX structure occurred for the area Y to X ratio of 2.8 and had a first natural frequency value of 596.36 rad/s. Contrary to the value of the first eigenfrequency, the XYXY periodic structure was characterized by higher values of the second eigenfrequency.

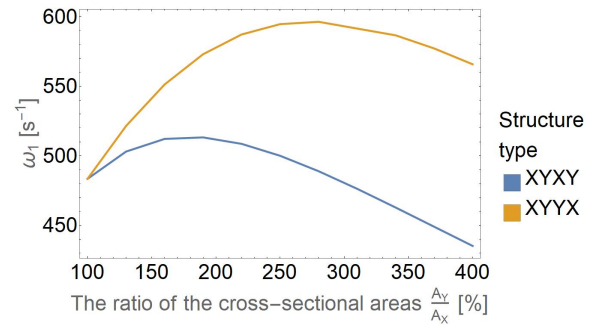


Fig. 2. The first eigenfrequency for binary (XYXY) and Thue-Morse (XYYX) structures depending on the ratio of the cross-sectional areas of segments Y to X

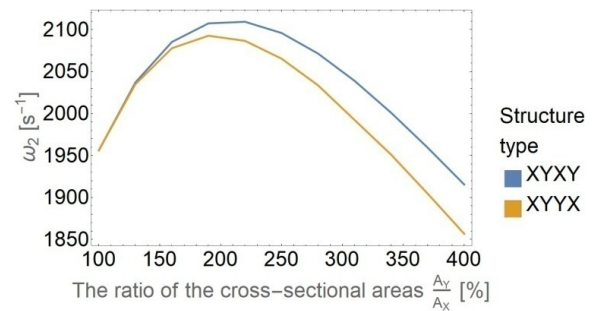


Fig. 3. The second eigenfrequency for binary (XYXY) and Thue-Morse (XYYX) structures depending on the ratio of the cross-sectional areas of segments Y to X

For the $\frac{A_Y}{A_X}$ cross-section ratio, both structures had maximum values of the second eigenfrequency, respectively for the XYXY structure $\frac{A_Y}{A_X} = 2.2$ and $\omega_2 = 2109.33$ rad/s and for the XYYX structure it was $\frac{A_Y}{A_X} = 1.9$ and $\omega_2 = 2092.69$ rad/s.

For both analyzed structures (Fig 4. And Fig. 5), there was an increase in dynamic stability with an increase in the A_Y cross-section, however, the XYYX structure showed a much higher dynamic stability than the XYXY structure. The studies have shown a significant impact of the stiffness distribution in the column on the natural frequency and dynamic stability for relatively simple structures.

4. Conclusions

The paper analyzes the impact of the stiffness distribution of the four-element Bernoulli-Euler beam for the periodic and aperiodic (Thue-Morse) systems on the first and second natural frequencies. Using the summation method and transforming the determined equations of motion into the form of the Mathieu equation, the change in dynamic stability of the examined structures was determined. It should be noted that the periodic structure showed higher values of the first eigenfrequency and lower values of the second eigenfrequency than the aperiodic structure.

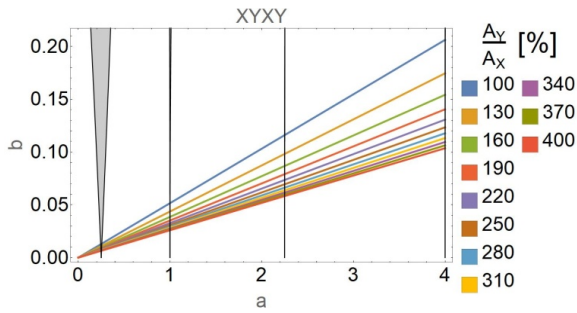


Fig. 4. Influence of the ratio of the cross-sectional areas of segments Y to X on the parameters a and b of the Mathieu equation for the binary structure (XYXY)

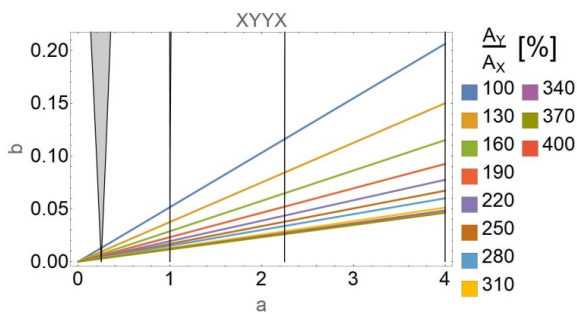


Fig. 5. Influence of the ratio of the cross-sectional areas of segments Y to X on the parameters a and b of the Mathieu equation for the Thue-Morse structure (XYYX)

All the analyzed eigenvalues were characterized by the maximum occurrence in the given range of changes in the A_Y cross-section.

As the ratio of $\frac{A_Y}{A_X}$ cross-sections increased in both structures,

the dynamic stability increased, although the XYYX structure was much more stable.

Acknowledgements

This publication was financed by the Ministry of Science and Higher Education of Poland as the statutory financial grant of the Department of Mechanics and Machine Design Fundamentals of Czestochowa University of Technology. The project is co-financed by the Governments of Czechia, Hungary, Poland and Slovakia through Visegrad Grants from International Visegrad Fund. The mission of the fund is to advance ideas for sustainable regional cooperation in Central Europe.

REFERENCES

- [1] Y.K. Lin, G.Q. Cai, Probabilistic structural dynamics, McGraw-Hill, New York (1995).
- [2] L.D. Landau, E.M. Lifshitz, Mechanics, Elsevier, Oxford (2007).
- [3] J.J.H. Brouwers, Physica D **240** (12), 990-1000 (2011). DOI: <https://doi.org/10.1016/j.physd.2011.02.009>
- [4] A.H. Nayfeh, D.T. Mook, Nonlinear oscillations, Wiley, New York (1979).
- [5] D. Yurchenko, A. Naess, P. Alevras, Probabilist. Eng. Mech. **31**, 12-18 (2013). DOI: <https://doi.org/10.1016/j.probengmech.2012.10.004>
- [6] Z.H. Feng, X.J. Lan, X.D. Zhu, Int. J. Nonlin. Mech. **42** (10), 1170-1185 (2007). DOI: <https://doi.org/10.1016/j.ijnonlinmec.2007.09.002>
- [7] G. Song, V. Sethi, H.-N. Li, Eng. Struct. **28** (11), 1513-1524 (2006). DOI: <https://doi.org/10.1016/j.engstruct.2006.02.002>
- [8] C.-Y. Lin, L.-W. Chen, J. Sound. Vib. **267** (2), 209-225 (2003). DOI: [https://doi.org/10.1016/S0022-460X\(02\)01427-X](https://doi.org/10.1016/S0022-460X(02)01427-X)
- [9] W. Sochacki, Thin Wall. Struct. **45** (10-11), 927-930 (2007). DOI: <https://doi.org/10.1016/j.tws.2007.08.023>
- [10] Y. Li, S. Fan, Z. Guo, J. Li, L. Cao, H. Zhuang, Commun. Nonlinear. Sci. **18** (2), 401-410 (2013). DOI: <https://doi.org/10.1016/j.cnsns.2012.06.025>
- [11] Y. Zhou, Y. Zhang, G. Yao, Compos. Struct. **267**, 113858 (2021). DOI: <https://doi.org/10.1016/j.compstruct.2021.113858>
- [12] W. Sochacki, J. Sound. Vib. **314** (1-2), 180-193 (2008). DOI: <https://doi.org/10.1016/j.jsv.2007.12.037>
- [13] Y.-S. Shih, Z.-F. Yeh, Int. J. Solids. Struct. **42** (7), 2145-2159 (2005). DOI: <https://doi.org/10.1016/j.ijsolstr.2004.09.007>
- [14] G.N. Jazar, Int. J. Nonlin. Mech. **39** (8), 1319-1331 (2004). DOI: <https://doi.org/10.1016/j.ijnonlinmec.2003.08.009>
- [15] A.A. Prikhodko, A.V. Nesterov, S.V. Nesterov, Procedia Engineer. **150**, 341-346 (2016). DOI: <https://doi.org/10.1016/j.proeng.2016.06.715>
- [16] M.J. Smyczynski, E. Magnucka-Blandzi, Thin-Wall. Struct. **113**, 144-150 (2017). DOI: <https://doi.org/10.1016/j.tws.2016.11.024>
- [17] Y. Fu, J. Wang, Y. Mao, Appl. Math. Model. **36** (9), 4324-4340 (2012). DOI: <https://doi.org/10.1016/j.apm.2011.11.059>
- [18] Y. Huang, J. Fu, A. Liu, Compos. Part B-Eng. **164**, 226-234 (2019). DOI: <https://doi.org/10.1016/j.compositesb.2018.11.088>
- [19] P. Sourani, M. Hashemian, M. Pirmoradian, D. Toghraie, Mech. Mater. **145**, 103403 (2020). DOI: <https://doi.org/10.1016/j.mechmat.2020.103403>
- [20] A. Talimian, P. Béda, Eur. J. Mech. A-Solid. **72**, 245-251 (2018). DOI: <https://doi.org/10.1016/j.euromechsol.2018.05.013>
- [21] H.-C. Li, L.-L. Ke, Thin-Wall. Struct. **161**, 107432 (2021). DOI: <https://doi.org/10.1016/j.tws.2020.107432>
- [22] M.A.R. Loja, J.I. Barbosa, C.M. Mota Soares, Compos. Struct. **182**, 402-411 (2017). DOI: <https://doi.org/10.1016/j.compstruct.2017.09.046>
- [23] S. Garus, W. Sochacki, J. Appl. Math. Comput. Mech. **17** (4), 19-24 (2018). DOI: <https://doi.org/10.17512/jamcm.2018.4.03>
- [24] C.S. Ryu, G.Y. Oh, M.H. Lee, Phys. Rev. B **48** (1), 132-141 (1993). DOI: <https://doi.org/10.1103/PhysRevB.48.132>
- [25] J.X. Zhong, J.R. Yan, J.Q. You, J. Phys.-Condens. Mat. **3** (33), 6293-6298 (1991). DOI: <https://doi.org/10.1088/0953-8984/3/33/008>
- [26] M. Kolář, M.K. Ali, F. Nori, Phys. Rev. B **43** (1), 1034-1047 (1991). DOI: <https://doi.org/10.1103/PhysRevB.43.1034>
- [27] H. Ni, J. Wang, A. Wu, Optik **242**, 167163 (2021). DOI: <https://doi.org/10.1016/j.ijleo.2021.167163>
- [28] Y. Trabelsi, N. Ben Ali, F. Segovia-Chaves, H.V. Posada, Results Phys. **19**, 103600 (2020). DOI: <https://doi.org/10.1016/j.rinp.2020.103600>